S.P. Todd, Z.A. Adamu, M.J. Cook and A.D.F. Price (2014) Natural personalised ventilation for hospital wards: Experimental validation, CIBSE ASHRAE Technical Symposium, Dublin, Ireland, 3-4 April 2014.

Natural personalised ventilation for hospital wards: Experimental validation

S.P. Todd*, Z.A. Adamu, M.J. Cook and A.D.F. Price
School of Civil and Building Engineering, Loughborough University, LE11 3TU, UK
* S.P.Todd@lboro.ac.uk

Abstract

Personalised ventilation (PV) systems are useful in protecting vulnerable hospitalised patients from airborne infection due to localised delivery of clean air. A natural personalised ventilation (NPV) system has previously been shown to be a feasible, natural and low-energy alternative to mechanised PV systems. The original NPV system was investigated using three conceptual designs which used dynamic thermal modelling and steady-state computational fluid dynamics to simulate a single-bed hospital ward. Findings from these designs led to optimisation of the NPV system components (stack and ducts) which also serve as the basis for this experimental validation. The objective of this research is to validate the flow characteristics of the optimised NPV system using scaled model experiments in addition to computational fluid dynamics (CFD) studies. Water-bath modelling (WBM) was carried out in a large Perspex tank and a scaled version of the single-bed ward was also constructed in Perspex. Results improve our understanding of the proposed NPV strategy, in particular showing that different locations of heat sources within the model leads to considerably different internal temperatures at steady state. Close similarities between CFD and WBM simulations were also observed.

Key words: natural personalised ventilation, buoyancy, flow visualisation, water bath modelling, computational fluid dynamics, kinematic similarity.

Introduction

Traditionally, naturally ventilated (NV) buildings are designed in such a way to provide sufficient fresh air to a room, with little or no thought to the location of the occupants. As a result, while sufficient fresh air may be delivered to the room, the occupants, due to their location, may not actually receive sufficient fresh air. Natural Personalised Ventilation (NPV) is a strategy where the ventilation design attempts to provide fresh air directly to the occupants within the space, instead of just to the room. Such a design was successfully demonstrated for hospitals by Adamu et al. (2011), using dynamic modelling (zonal airflow) and steady state computational fluid dynamics (CFD). Both of these numerical methods are widely used in research and industry, ensuring conservation of mass, energy, momentum and chemical and biological species (Chen, 2009; Li and Nielsen, 2011). Computer simulations, whilst a very powerful tool, is subject to its assumptions, and to the equations which they use. As a result, comparing the results from computer simulations with experimental techniques allows for validation between both simulation techniques.

Since Linden et al (1990) produced natural ventilation theory and showed that the theory closely agreed with the interface heights and densities above interface heights recorded in the water-bath modelling (WBM) simulations, WBM has been used to improve our understanding of natural ventilation as well as to simulate complicated and novel scenarios. Despite providing less quantitative information than computational simulation, the greatest

strength of WBM lies in its ability to show how air flows develop. WBM is further described in section 2.

The design of the NPV system being validated is illustrated in Fig. 1. A duct allows fresh air to flow into the room and is positioned just above the bed. A stack is positioned at the edge of the room. The objective of this paper is to use WBM to simulate the NPV strategy discussed in Adamu et al. (2011), compare results and airflow characteristics between WBM and computer simulations, whilst also discussing the effect that different locations of heat sources have on the thermal environment within the space.

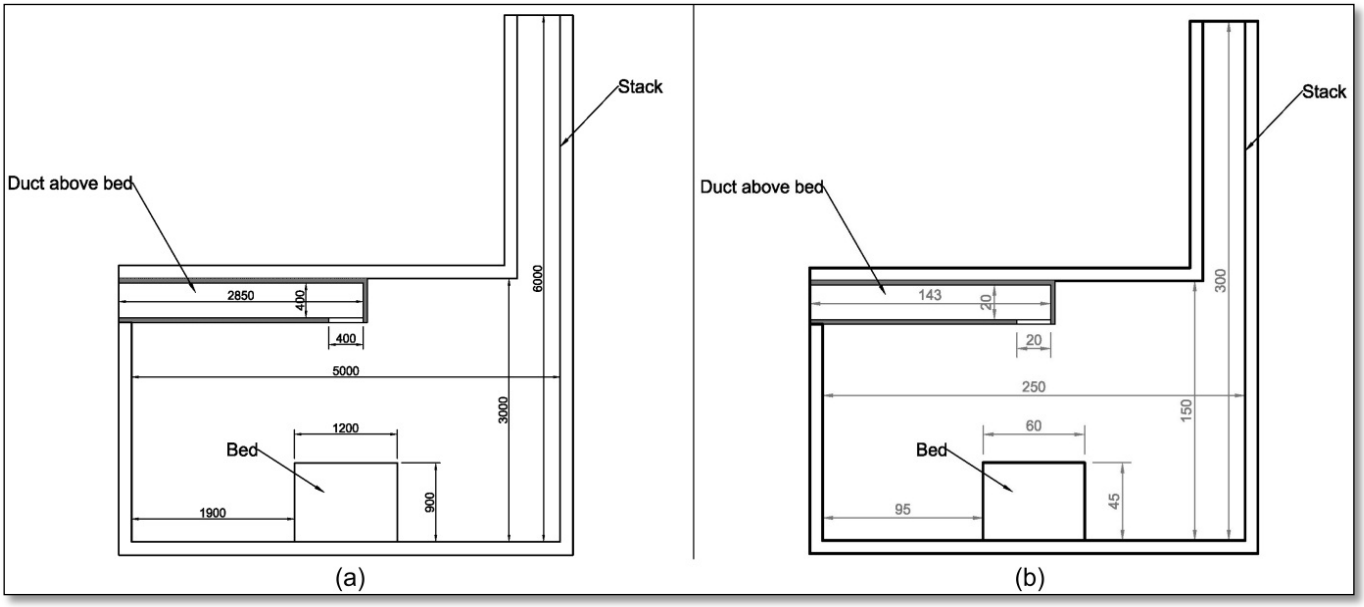

Figure 1: Internal dimensions of (a) ward at scale 1:1 and (b) the Perspex model at scale 1:20

2.0 Materials and modelling procedure

A model of the hospital ward was constructed out of Perspex to a scale of 1:20 (Fig. 2a). Brine coloured with food dye (to aid the visualisation of the flow) is used to create density differences with 'fresh' water in order to simulate the density differences between hot air, and ambient temperature air. The brine is released into the model via nozzles which are based on the design used in several other WBM experiments including those of Hunt and Linden (2001).The nozzle design, with a 0.5cm diameter outlet and the 200µm mesh within the nozzle encourages a turbulent plume to form, allowing the virtual origin (Hunt and Kaye 2001) of the plume to be calculated. The Perspex model was suspended (Fig. 2b) within a large Perspex water tank (Fig. 2c) measuring 1.5 x 1 x 2m approximately 300mm below the surface of the water.

The brine was pre-prepared in a storage tank (Fig. 2d), with the density of the brine measured using an Anton Parr Portable DMA 35 density meter with an accuracy of 0.001 g/cm^3. It was then pumped into a header tank, which maintained a constant head by incorporating an overflow pipe which fed back into the storage tank keeping the brine within the storage tank

well mixed. The brine was then gravity fed into the nozzle within the Perspex model, with the flow rate controlled by an inline analogue flow meter. The volume of water within the tank (Fig. 2c) is such that if a simulation ran for 30 minutes with a flow rate of brine into the model of 2 cm3/s, the depth of water within the tank would increase by 2.3mm. This is deemed sufficiently small such that there would be a negligible effect on WBM simulations.

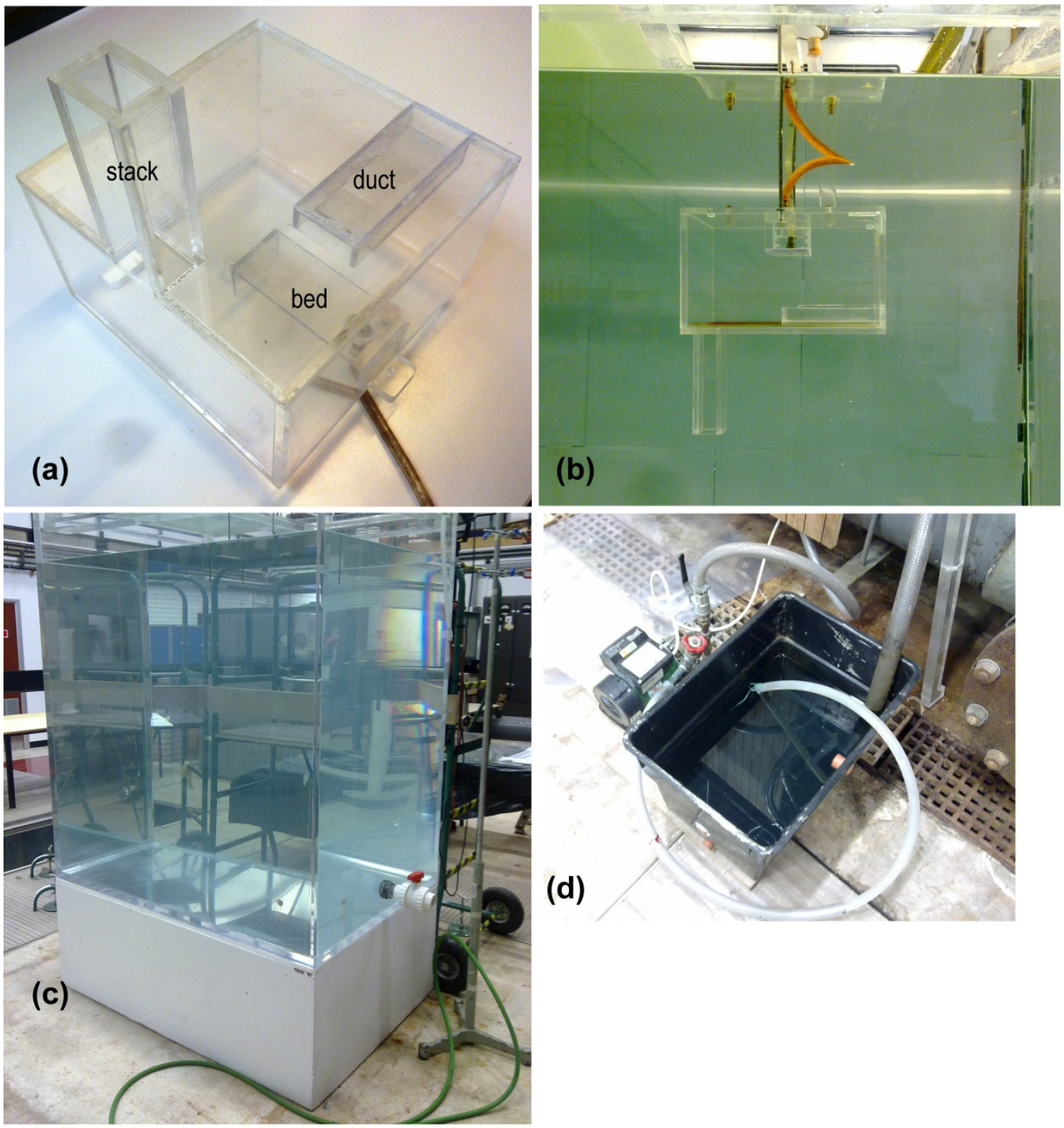

Figure 2: Experimental set up showing (a) scaled model (b) inverted and immersed model (c) water tank (d) brine container

Heat sources in several different locations within the model were simulated (Figure 3). A patient was simulated on the bed (1), with position 2 at the foot of the bed and positions 3 & 4 on either side of the bed representing visitors and hospital staff. All four heat sources were

represented as point heat sources. Even though this is strictly not true for the patient who would likely be laid on the bed, the simplification was deemed acceptable.

Photographs and recordings were taken during experiments to record the transient flows for analysis. Two conductivity probes were used within the model to measure conductivities throughout the simulations. Both were Oakton CON 11 handheld conductivity meters with minimum resolution of 0.1 mS. One probe was placed at low level whilst another was placed at high level within the model. Density of the water within the tank but outside of the model was also measured to ensure that it remained constant throughout all simulations.

Brine is used to represent a heat source, however because it is denser than the 'fresh' water representing ambient temperature air, the brine will sink to the bottom. As a result, the model is turned up-side-down, so that heat sources are located at the top of the model (where the floor of the room is located), and an interface forms at the bottom of the model (where the ceiling of the room is located).

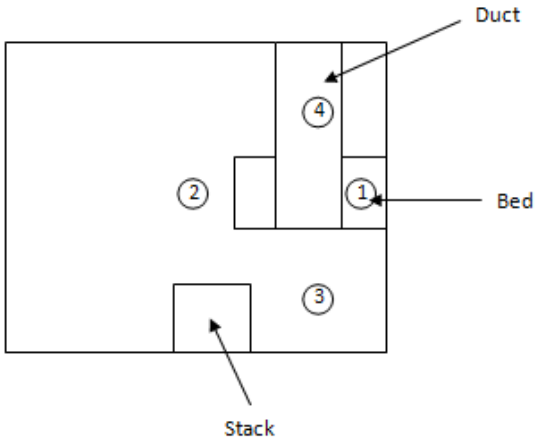

Figure 3. Plan view of hospital model with number locations of heat sources.

3.0 Scaling method

In order to ensure that the WBM simulation is accurately representing the real life scenario that we wish to simulate, the model's dimensions must be scaled to the real life room dimensions. Next, kinematic similarity between the model and the real life scenario is required. To achieve Kinematic similarity, Prandtl numbers (Pr – ratio of viscous diffusion and thermal diffusion), Reynolds numbers (Re – ratio of inertial forces and viscous forces), and Archimedes numbers (Ar – ratio of buoyancy forces to inertial forces) should be made equal between the model and full scales (H. Awbi 2003). Because the fluid changes between full scale and model scale (Air to water), it is impossible to match Pr, however it is possible to match Re and Ar and this is noted in other research as being acceptable (Walker 2006). Subscripts 'm' and 'f' refers to model and full scale values.

$$Re_m = Re_f \frac{\sqrt{g'_m H_m} H_m}{\nu_m} = \frac{\sqrt{g'_f H_f} H_f}{\nu_f} \quad (1)$$

$$Ar_m = Ar_f \frac{gH_M^3\rho_m(\Delta\rho_m)}{\mu_m} = \frac{gH_f^3\rho_f(\Delta\rho_f)}{\mu_f} \quad 2$$

$$Pr_m = Pr_f \frac{\nu_m}{\alpha_m} = \frac{\nu_f}{\alpha_f} \quad 3$$

Where ν is the kinematic viscosity (m^2/s), μ is the dynamic viscosity (kg/m.s) and α is the thermal diffusivity (m^2/s). By calculating the Reynolds number and the Archimedes number for the reduced scale simulation, the equations can be re-arranged to calculate g'_f or $\Delta\rho_f$.

To ensure that $Re_m = Re_f$ and $Ar_m = Ar_f$, a four-step Iterative procedure was followed and is described below. Subscripts m refers to values for 'model scale', while f refers to values in 'full scale'. Following this procedure will ensure that the flow within the model closely follows air flow at full scale.

Step 1: Calculate the Archimedes (Ar) and Reynolds (Re) numbers for the scaled model
The Effective Opening Area (A*) of the model needs be calculated and is found using Equation 4 which is provided by Linden (1990) as:

$$A_m^* = \frac{a_1 a_2}{\sqrt{0.5\left(\frac{a_1}{cd_1}\right)^2+\left(\frac{a_2}{cd_2}\right)^2}} \quad 4$$

Where Cd is the discharge coefficient to account for vena contracta through openings a_1 at low level and a_2 at high level. In order to achieve kinematic similarity, initial values for density of the brine, ρ and flow rate, $F_{o,m}$ must be chosen. These values will likely be changed later on in this four step process. The buoyancy of brine plume B_m, is calculated using Equation 5:

$$B_m = F_{o,m}g'_m = F_{o,m}g\frac{\rho_o-\rho}{\rho} = F_{o,m}g\frac{T_o-\Delta T}{T} \quad 5$$

Where subscript 'o' denotes initial values of brine before it enters the scaled model, ρ is the density of the ambient fluid (Kg/m^3) and T is the ambient temperature of the ambient fluid (K). To calculate the approximate interface height to be observed within the scaled model, h, the ratio between effective opening area (A_m) and the height between the heat source (including the virtual origin) and outlet (H^2_m) was utilised (Linden 1990) as shown in Equation 6.

$$\frac{A_m^*}{H_m^2} = C^{\frac{3}{2}}\sqrt{\frac{\left(\frac{h_m}{H_m}\right)^2}{1-\left(\frac{h_m}{H_m}\right)}} \quad 6$$

The reduced gravity (g') of the brine below the interface can then be computed using Equation 7.

$$g' = \frac{(B_m{}^2 h_m{}^{-5})^{\frac{1}{3}}}{C} \quad 7$$

Where C is a constant derived in Morton, et al. 1956 and can be taken to be 0.158.

The source Archimedes equation to account for the addition of brine into the space (Hunt et al 2001) shown as Equation 8:

$$Ar_m = \left(\frac{\frac{F_{o,m}}{\sqrt{\frac{F_{o,m}{}^2}{A_n}}}}{\frac{\left(\frac{F_{o,m}{}^2}{A_n}\right)^{\frac{3}{4}}}{\sqrt{B}}} \right)^2 \quad 8$$

Where A_n is the area of the nozzle where the brine enters the scaled model.
When Ar =1, flow is driven by buoyancy instead of by momentum (Walker 2006).
The Reynolds number for the scaled model (Re_m) was then calculated using Equation 1.

Step 2: Equal the Ar and Re between scaled model and full scale

Equation 6 can thus be re-arranged to calculate the reduced gravity at full scale, g'_f. The Archimedes number for the full scale will always equal 1 providing that there is no wind, or induced momentum/velocity on the hot air plume, so Ar_m must be made approximately equal to 1, which is achieved in Step 4.

Step 3: Calculate the buoyancy of hot air plume in full scale building

Having calculated the reduced gravity of hot air above the interface in the full scale building, g'_f , the temperature of the hot air above the interface is calculated using Equation 9 , where T is the ambient temperature in Kelvin.

$$\Delta T = \frac{g'_f T}{g} \quad 9$$

The Buoyancy of the plume is then calculated through Equation 10.

$$B = \sqrt{\frac{\left(g'_f C\right)^3}{h_f^{-5}}} \quad 10$$

Where h_f is calculated using equation 11 (Y. Li 2000)), because equation 6 does not take into account surface radiation which is experienced at full scale but not in water bath simulations using brine), resulting in an under prediction of the interface height for air.

$$\frac{A*}{H^2} = C^{\frac{3}{2}} \sqrt{\frac{\frac{h_f}{H_f}}{1-(1-\lambda)\frac{h_f}{H_f}}} \quad 11$$

Where λ is a temperature coefficient which is determined by the convective heat transfer at the floor and ceiling of the room, and the radiative heat transfer coefficient and is generally around 0.4 for natural displacement flows (Li 2000).

Step 4: Calculate the equivalent heat output at full scale being simulated in Water Bath

Equation 12 was re-arranged to make watt of heat source, W, the subject of formula:

$$B = \frac{Wg\alpha}{\rho_f Cp} \quad 12$$

This was then applied to calculate the wattage of the heat source in the full sized room by having calculated the buoyancy of the plume within the room. Where α is the thermal expansion coefficient, and Cp is the specific heat capacity.

Changing the values of $F_{o,m}\Delta\rho_m$ and H_m will change R_{em}, A_{rm}, and W. The values should be changed until A_{rm} is approximately equal to 1, and the brine plume was representing the desired heat source. It is possible that even after saturating water with salt, increasing the flow rate substantially, while also making large changes to H_m, the desired W cannot be achieved. In such cases, applying a small multiplier to Re_m when using equation 6 to calculate the reduced gravity at full scale may be required. While this means that R_{em} and R_{ef} will no longer be equal, a previous study (Gladstone and Woods, 2001) suggested that similarity between model and full scale can be achieved if the difference in the values of R_{ef} and R_{em} are one order of magnitude apart. Etheridge and Sandberg (1995) suggest that not being able to achieve similarity with all three dimensionless numbers is acceptable providing that the flow is fully turbulent ($Re > 2.3 \times 10^3$) however CIBSE guide C states that flow is only fully turbulent when $Re > 3 \times 10^3$. Whilst other studies state that flows at model scale should have high Reynolds (10^4 or higher) numbers so that viscous effects are negliable and advection dominates molecular diffusion (Fitzgerald 2013, Hunt and Coffey 2010).

4 Results and discussion

Several simulations were run within the model and in all cases, densities at high and low level were measured by conductivity probes. Firstly, scenarios are run and observed flows are compared with CFD predictions. Then, the densities at high and low level are compared between the WBM scenarios till steady state is reached. Each simulation was run 5 times to ensure repeatability of results.

4.1 Observed flow behaviour

The density of brine in each case was 1.100 g/cm^3, and the flow rate of the brine flowing into the model through the nozzle was 120 cm^3/min. Both parameters were calculated using the methodology in section 3.1 to ensure that the model was simulating a 50W heat source. A multiplier of 6.5 had to be applied to Re_m in Step 4 of section 3. When the brine was allowed to flow into the model, it exited the nozzle fully turbulent, and so began entraining ambient fluid (fresh water). The brine plume reached the bottom of the model and began to horizontally spread outwards (Fig. 4a). The brine at the bottom of the model began to build up (Fig. 4b) to a point where an interface began to form (Fig. 4c).

Shortly after the interface had stopped rising, the water above the interface began to turn light shades of blue (the colour of the dye used in the brine). This happened because the inlet duct was below the interface, the incoming 'fresh' water mixed with the brine, before rising into the space near the bed. The area above the interface continued to darken for some time after the interface had stopped rising. This means that for a real hospital room using this ventilation technique, the fresh air is pre-warmed before coming into contact with the patient, reducing the chance of thermal discomfort due to draughts, while also potentially reducing heating requirements during winter.

However, this mixing of incoming air with warm air at high level within the space may increase the risk of infection to patients within the space if the ventilation system is used for rooms with more than one patient. The intention of the incoming air to flow onto the patient is to reduce air from other patients in the form of coughs and sneezes being breathed in by the patient due to positive air pressure in the vicinity around the patient. This idea of positive air pressure to reduce infection is used in hospital rooms where surgeries take place. However, in this scenario, because the incoming air mixes with air that may contain particulates from other patients coughs and sneezes, it becomes possible for patients to become infected. To prevent this, the duct height must be reduced such that it is below the interface. However, the trade-off being will be increased heating requirements.

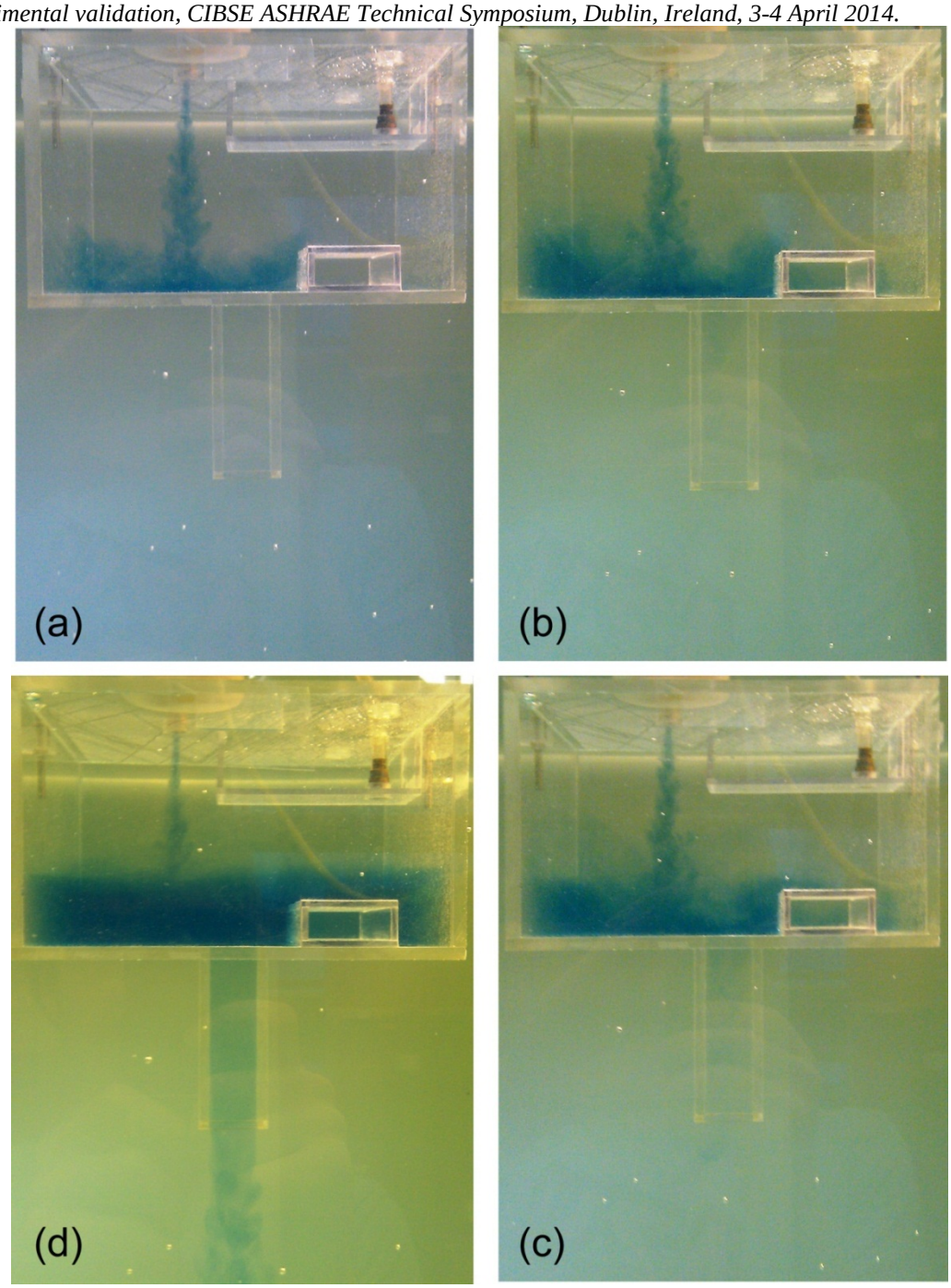

Figure 4: Transitional development of internal thermal environment shown in clockwise direction from (a) initialisation to (d) attainment of maximum interface height. All views looking through the NPV duct which remains free of brine. This simulation had one heat source located at position 2.

Buoyancy forces within the model draw ‘fresh’ water into the duct, and exiting fresh water from the duct has horizontal momentum (caused by travelling horizontally through the duct) and a vertical force due to density differences. The combined result is that the incoming fluid travels diagonally, as shown in Fig 5. The horizontal momentum actually causes the fresh water to travel past the bed, instead of landing onto the bed. To achieve air flow from the duct landing on the bed, the duct outlet should be positioned offset from the bed to allow for

horizontal displacement of the 'fresh' water. However, the horizontal force acting on the 'fresh' water as it travels through the duct will vary depending on the buoyancy forces within the room. As a result, offsetting the duct outlet may not always achieve air flow onto the patient.

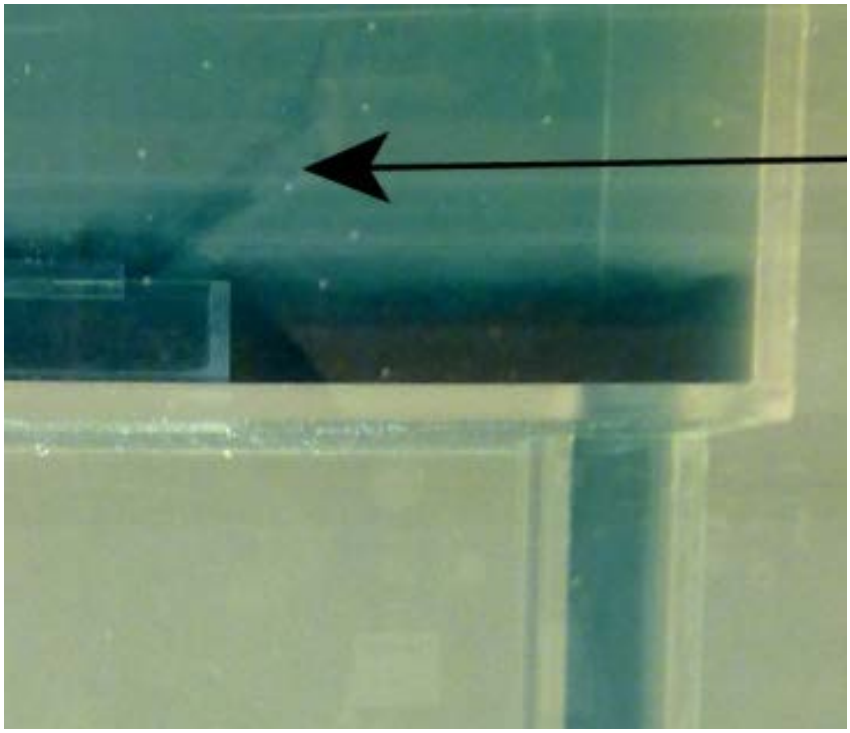

Figure 5. The scaled model at steady state (arrow indicates flow of fresh air from the duct) for the scenario where there is one heat source at position 1.

4.2 Comparison with CFD: Interface height and interesting fluid flows.

Experimental and CFD simulations are compared for the scenario where the only heat source in the room is a patient in the bed. The interface height in the Perspex model came to approximately 13cm from the floor of the model, with CFD simulations (Fig. 6) and the analytical model described in 2.1 in close agreement (13.06 cm). The difference in interface height between this scenario, and the scenario described in 4.1 is due to the difference in height between the two heat sources (4cm). Interestingly, the interface height is just above the height of the duct opening where fresh fluid flows into the room. However, a build-up of brine (in WBM) and hot air (CFD) is observed (Fig. 7) behind the vent. This build up caused the fluid to flow over the duct opening.

As a result, the fluid coming into the room from the vent mixed with the overflowing brine/hot air, allowing for mixing ventilation to occur. Future ventilation designs could attempt to incorporate designs which allow for hot air to build up around and flow over an inlet to 'pre-warm incoming cold air.

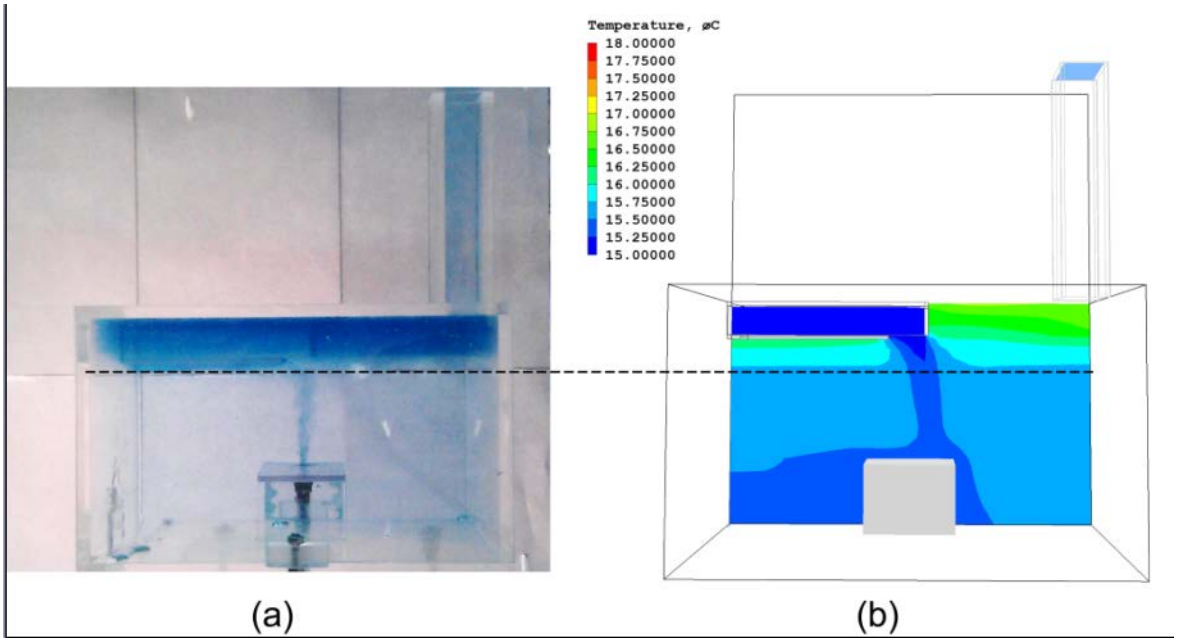

Figure 6: The interface layer in (a) WBM and (b) CFD equivalent. Fig. 6a has been rotated 180 degrees to aide in the comparison Fig. 6b.

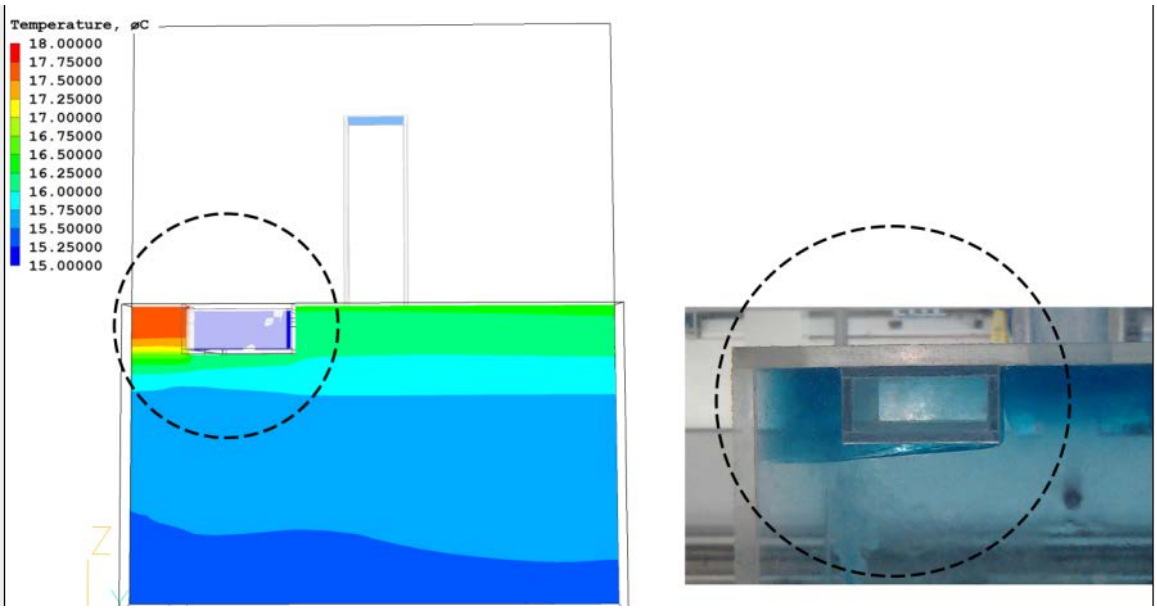

Figure 7: Formation of eddies around duct in (a) CFD and (b) WBM .Fig 7b has been rotated 180 degrees to allow for comparison with Fig. 7

4.3 Density comparisons before and during steady state

This section compares the density measurements made by the conductivity probes during the simulations. A measurement was made every 5 seconds and all simulations begin when a brine source is just turned on and were run till steady state was reached.

Figure 8 shows the density profiles at a) near the ceiling of the model and b) near the floor of the model for scenarios where each of the heat sources are individually turned on. It is interesting to note that there is considerable difference in density at both low level and high level between the four scenarios.

When the heat source is located at position 1, the temperature increase at both high and low level is the smallest when steady state is reached; while it is the largest for position 3. Position 2 and 4 achieve similar temperatures at high and low level. Most interesting, is the large variation in density measured for location 3 compared to the other scenarios. This significant variation and greater densities can be explained by the position of the heat source. As the density at high level increases, flow through the space increases. This results in a greater velocity being associated with the incoming fluid through the duct. The increased velocity means that the incoming fluid has greater penetration into the space. This increased penetration results in greater quantities of incoming fluid colliding with the brine plume at position 3. Mixing ensues, leading to the environment at low level increasing in temperature beyond the other scenarios. As the temperature at low level increases, the brine plume entrains fluid of greater density than in the other scenarios resulting in the plume becoming less diluted. This in turn results in the density at high level becoming greater than in the other scenarios. It is believed that the added turbulence of the incoming fluid colliding with the plume results in considerable variation in density at steady state.

Steady state temperature at high level was first reached for the scenario where only the patient was in the room (300s) while the other three scenarios took considerably longer (600s). Of note, steady state at low level is reached slightly more quickly for heat source locations 2, 3 and 4 (800s) while heat source location 1 took longer (1000s). The difference in times to reach steady state can be explained by the differences in height between position 1 and 2, 3 & 4. Position 1 sees an interface which is above the duct outlet. There are therefore no apparent complex air flows occurring until a build-up of brine occurs behind the duct. This results in incoming fluid mixing with some of the dense fluid within the space (figure 7). However, the incoming fluid interacts with a much smaller volume of dense fluid than in the other scenarios, causing an increase in density at low level which is much lower than the other scenarios. It is this slow build-up of brine at low level which results in the density at high level taking considerably longer to achieve steady state. By approximately 60s, the density at high level is 1.00045 kg/m3 and this slowly increases to 1.00055 kg/m3 by 300s.

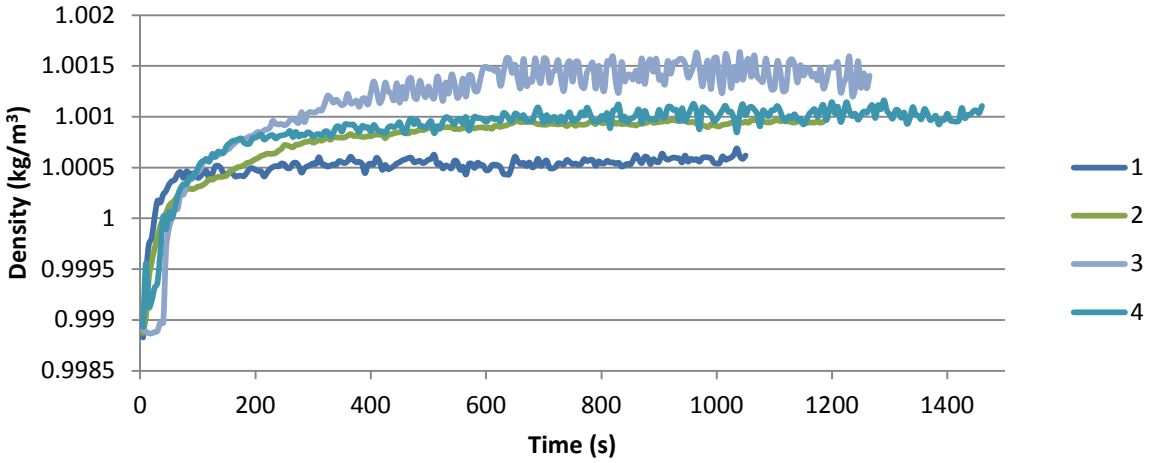

a)

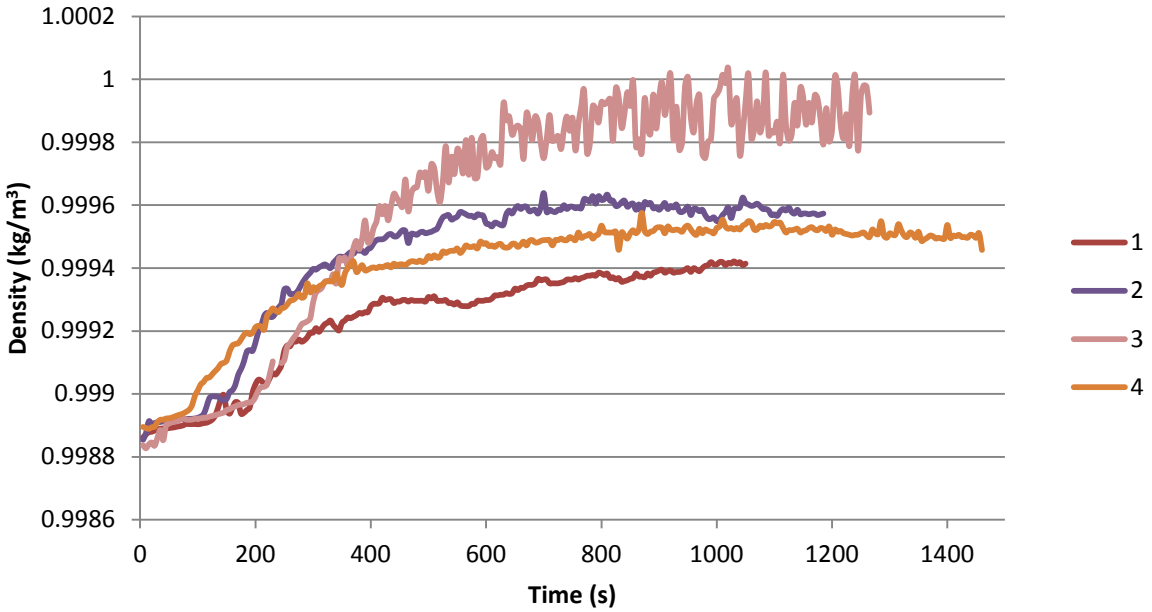

b)

Figure 8. Density profile for scenarios where individual heat sources are within the space where a) density recorded at high level and b) density recorded at low level.

5 Conclusion

This paper has conducted Water Bath Modelling simulations with a model which uses a novel natural ventilation strategy which intends to reduce cross infection between patients. This involves a stack which allows hot air to flow out of the room, with a high level duct allowing ambient air to flow into the room. Agreement has been shown for the flow regimes within the model between CFD and WBM simulations. Importantly, this paper sets out to further understand this ventilation technique and 4 simulations were conducted, each with different brine source locations. Densities were measured at high and low level within the model and it

was shown that with identical physical parameters between all simulations except the location of the heat source, significant variation in internal densities at low and high level occurs. The time to reach steady state within the model is also shown to vary. Such variation is caused by the interaction between the brine plume and the duct. For the scenario where a heat source is located such that direct interaction between incoming fluid and the brine plume occurred, significantly higher internal temperatures were observed. For the case where the patient is in the room only, lowest internal temperatures were observed and this is attributed to the duct opening not being above the interface. Interestingly, due to the location of the duct, a build-up of brine behind the duct was observed which caused brine to flow over the opening resulting in a mixed environment. This mixed environment reduces heating requirements for the room as incoming fluid is pre-warmed. However, the suitability for this strategy to reduce infection of patients is questionable unless the height of the duct is reduced to ensure that mixing between incoming fluid and stale air does not occur. For the three other scenarios, the duct opening was above the interface leading to a mixed environment as well. However this pre-warming may not be acceptable during summer when ambient temperatures are high.

References

Adamu ZA, Cook MJ, Price ADF (2011b). Natural Personalised Ventilation: A novel approach, International Journal of Ventilation, 10(3): 263-275.

Awbi H.B. (2003) Ventilation of Buildings, Second Edition, 2003, ISBN 0415270553, Taylor and Francis (E&FN Spon).

Chen, Q. (2009) Ventilation performance prediction for buildings: a method overview and recent applications, Building and Environment, 44 (4) (2009), pp. 848–858

CIBSE Guide C 2007 ISBN 9781903287804

Fitzgerald, Shaun (2013), The science of Water Bath Modelling. Last accessed on 20/11/2013. http://www.breathingbuildings.com/news/natural-ventilation-blog/the-science-of-water-bath-modelling?utm_medium=email&utm_campaign=Breathing%20Buildings%20September%202013&utm_content=Breathing%20Buildings%20September%202013+CID_9d693cdd4307adef29f957cd77df241d&utm_source=CplusNewsletter

Gladstone C, and Woods AW, 2001. On a buoyancy-driven natural ventilation of a room with a heated floor. J. Fluid Mech. (2001), vol. 441, pp. 293{314Etheridge and

Hunt G.R, and Linden P.F, 2001, Steady-state flows in an enclosure ventilated by buoyancy forces assisted by wind. J. Fluid Mech. (2001), vol 426, pp 355-386.

Hunt GR, Cooper P and Linden PF 2001. Thermal stratification produced by plumes and jets in enclosed spaces. Building and Environment 36 (2001) 871 – 882

Hunt G.R, and Kaye N. G, 2001. Virtual origin correction for lazy turbulent plumes. J. Fluid Mech. (2001), vol, 435, pp. 377-396.

Hunt G. R and Coffey, C. J. Emptying boxes – classifying transient natural ventilation flows j, Fluid Mech, (2010) vol 646 pp 137-168

Li Y, Buoyancy-driven natural ventilation in a thermally stratified one-zone building, Building and Environment 35 (2000) 207–214.

Li, Y. and Nielsen, P.V. (2011) CFD and ventilation research, Indoor Air, 21 (6) (2011), pp. 442–453

Linden PF, Lane-Serff GF, Smeed DA. 1990. Emptying filling spaces: the fluid mechanics of natural ventilation. J. Fluid Mech. 212:300–35

Morton BR, Taylor GI, Turner JS (1956). Turbulent gravitational convection from maintained and instantaneous sources. Proceedings of the Royal Society A 234:1-23

Sandberg, 1995. Etheridge. D and Sandberg, M. (1995) Building Ventilation: Theory and measurement, Wiley Press, New York.

Walker CE, 2005, Methodology for the Evaluation of Natural Ventilation in Buildings. Using a Reduced-Scale Air Model, Ph.D thesis, Massachusetts Institute of Technology